

# On the Transition State between the Oil–Water and Air–Water Interface

M. Harke and H. Motschmann\*

Max-Planck Institute of Colloids and Interfaces, Rudower Chaussee 5,  
D-12489 Berlin, Germany

Received August 20, 1997. In Final Form: October 21, 1997

Insoluble monolayers at the air–water interface are exposed to a gas phase containing organic hydrocarbons. The hydrocarbons are partly incorporated within the monolayer which leads to changes in orientational order and the formation of new phases of different morphology. The transition state resembles features of the air–water and oil–water interface and the control of the hydrocarbon partial pressure allows continuous tuning between both interfaces. The phospholipid D,L- $\alpha$ -dipalmitoylphosphatidylethanolamine, DPPE, and an ester diol hexadecanoic acid, 2,3-dihydroxypropyl ester, ESD-16, are used as amphiphiles, and pentane, *n*-hexane, cyclohexane, 2,2-dimethylbutane, *n*-heptane, *n*-decane, and *n*-dodecane are used as hydrocarbons. Both amphiphiles differ in their headgroup size. In DPPE the aliphatic tail determines the packing within the monolayer, but in the case of ESD-16 it is the headgroups. The structural changes are monitored by surface pressure–area ( $\pi$ ,*A*) isotherms and imaging ellipsometry. The influence of the chemical nature of the hydrocarbon and the effect of the partial pressure of the hydrocarbon on the monolayer structure are assessed.

## 1. Introduction

The oil–water interface plays a decisive role in many aspects of daily life. Despite its importance, still little is known about the organization of amphiphiles at this interface and their corresponding static and dynamic interfacial properties.<sup>1</sup> This is mainly due to severe restrictions on the analytical tools imposed by this buried interface. Many powerful techniques suitable for investigating the liquid–air interface such as X-ray reflectometry or X-ray diffraction cannot be applied at liquid–liquid interfaces. X-ray diffraction in particular has provided a new insight into the organization of insoluble monolayers at the air–water interface.<sup>2</sup> These measurements allow determination of the lattice structure within different phases and provide corroborative evidence for the fairly complex phase diagrams as retrieved by surface tension measurements.<sup>3</sup> Unfortunately this powerful technique is not available for investigation of the macroscopic oil–water interface.

The present paper focuses on a transition state between the macroscopic oil–water and the air–water interfaces. The common theme of the following set of experiments is as follows: A monolayer of a water insoluble amphiphile is exposed to a gas phase containing organic hydrocarbons at a well-defined partial pressure. The hydrocarbon interacts with the monolayer and is incorporated, leading to changes in the orientational order, lattice structure, and morphology. As a result, a transition state evolves, which resembles features of both the bare air–water as well as the macroscopic oil–water interface. The control of the partial pressure of the hydrocarbon allows a detailed assessment of structural changes from the air–water to the macroscopic oil–water interface. The present study focuses on this intermediate state and utilizes mainly surface tension measurements for the determination of  $\pi$ ,*A*-isotherms and imaging ellipsometry for the visualiza-

tion of the morphology on an mesoscopic length scale. This transition state can also be investigated by all analytical tools available for the bare air–water interface. X-ray diffraction data on this system will be discussed in a future contribution of ours.

The manipulation of organic monolayers via the gas phase has been widely ignored compared to the numerous studies dealing with the influence of the subphase on a monolayer.<sup>4,5</sup> The subphase properties have been changed by dissolving salts, by pH changes, or by adding soluble surfactants. Previous studies on the influence of the gas phase on monolayers included investigations of the influence of argon, xenon, and nitrogen. However, these inert gases had no impact on the monolayer.<sup>5</sup> The adsorption of hydrocarbons on the bare water interface was investigated by Baumer et al.,<sup>6</sup> and the decrease in the surface tension provided evidence of the adsorption of hydrocarbons at the bare water surface. This arrangement is now used for fundamental wetting studies in order to retrieve the nature of the underlying forces driving wetting phenomena.<sup>7</sup>

A monolayer of an insoluble amphiphile at the air–water provides additional adsorption sites for hydrocarbons from the gas phase. This process was first studied by Dean et al. using surface tension measurements,<sup>8</sup> and on the basis of a phenomenological thermodynamic model, the number of molecules incorporated in the monolayer was estimated.

Clements et al.<sup>9</sup> and Ueda et al.<sup>10</sup> used the same arrangement to study aspects of the interaction of volatile narcotics on the cell membrane using Langmuir films as simple models for the latter. Also chemical reactions of Langmuir monolayer with molecules from the gas phase have been investigated, e.g., Lai et al. studied the reac-

\* To whom correspondence should be addressed: electronic mail, motschma@mpikg.fta-berlin.de.

(1) Möhwald, H. *Rep. Prog. Phys.* **1993**, *56*, 653.

(2) Möhwald, H. *Annu. Rev. Phys. Chem.* **1990**, *41*, 441.

(3) Knobler, Ch. *Annu. Rev. Phys. Chem.* **1992**, *43*, 207.

(4) McConnell, H. M. *Annu. Rev. Phys. Chem.* **1991**, *42*, 171.

(5) Gaines, G. L. *Insoluble Monolayer at liquid gas interfaces*; Wiley: New York, 1996.

(6) Baumer, D. Findenegg, G. J. *Colloid. Interface Sci.* **1981**, *85*, 118.

(7) Pfohl, T.; Möhwald, H.; Riegler, H. *Langmuir*, in press.

(8) Dean, R. B. *Kolloid Z.* **1953**, *123*, 117.

(9) Clements, J. A.; Wilson, K. M. *Physiology* **1965**, *48*, 1009.

(10) Ueda, J.; Shieh, D. D.; Eyring, H. *Anesthesiology* **1974**, *41*, 217.

tion of unsaturated phosphocholins at the air–water interface with ozone.<sup>11</sup>

Recent studies on the oil–water interface deal with mixtures of long chain alkanes and monolayers of amphiphiles in order to retrieve models of the molecular organization of amphiphiles. Thoma et al. studied the influence of long chain alkane droplets in contact with monolayers of phospholipids. The incorporation of hydrocarbon caused a significant change in orientation of the amphiphiles.<sup>12</sup> However, this geometry appears to be ill defined because of intrinsic concentration gradients. Aveyard et al. added oil droplets to aqueous solutions of soluble surfactants<sup>14</sup> and found correlations between phase behavior of microemulsions and monolayer.<sup>15</sup>

Obviously, the interaction of a monolayer with a gas phase conveys a couple of interesting features and provides a better understanding of molecular organization of amphiphiles at the air–water and oil–water interface. The experimental arrangement used in the present contribution is well defined compared to studies using oil droplets in contact with the monolayer. The interaction of the molecules of the gas phase with the monolayer is homogeneous in time and space and offers the possibility to deliberately control the partial pressure of the hydrocarbon. In addition, with our arrangement all established surface analytical tools used for the air–water interface can be applied.

Two different amphiphiles are used in the following study, the phospholipid *D,L*- $\alpha$ -dipalmitoylphosphatidylethanolamine, DPPE, and hexadecanoic, 2,3-dihydroxypropyl ester, ESD-16 (see Figures 3 and 4). Both compounds have been thoroughly studied at the air–water interface by various groups and there is a profound understanding of their phase diagrams, morphology, and lattice structure.<sup>2,13</sup> A striking difference between both components is the ratio of the diameter of aliphatic tail to its headgroup size. The aliphatic tails determine the packing within the DPPE monolayer, whereas in the case of the ESD-16 the headgroup determines the packing. The corresponding monolayers differ in their free volume and thus the choice of materials addresses two extreme cases.

## 2. Experimental Section

**2.1. Experimental Arrangement.** Figure 1 illustrates the experimental arrangement used. A conventional Langmuir trough equipped with a Wilhemy balance (R&K1, Riegler & Kirstein GmbH, FRG) is placed in an air-tight housing of volume 14 dm<sup>3</sup>. A nitrogen stream of flow rate 4 dm<sup>3</sup>/h is flushed through a set of gas washing bottles containing hydrocarbon and water. The latter ensures a constant water level within the trough during the course of the experiment. The partial pressure of the hydrocarbon is adjusted by the temperature of the hydrocarbon. The prevailing surface pressure was calculated with the aid of the Antoine equation.<sup>16</sup> Valves allow pure nitrogen to be flushed through the system to create well-defined initial conditions and to investigate also the reversibility of all processes. Measurements at

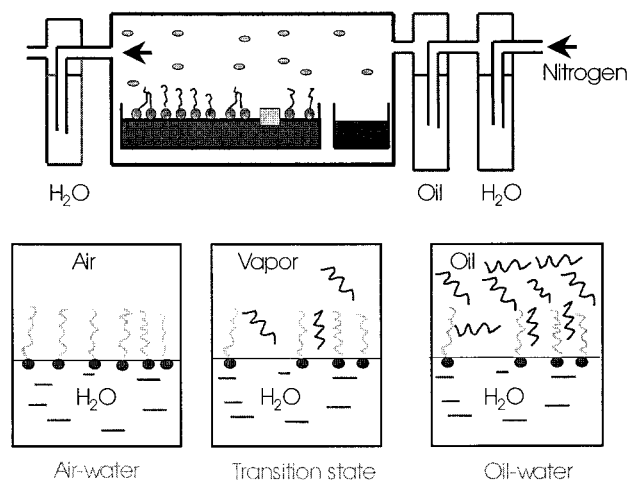


**Figure 1.** Sketch of the experimental setup. A conventional Langmuir trough equipped with a Wilhemy balance is placed in an air-tight housing. A nitrogen stream is flushed through a set of gas washing bottles containing hydrocarbon and water. The latter ensures a constant water level within the balance during the course of the experiment. The partial pressure of the hydrocarbon is adjusted by the temperature of the hydrocarbon. Valves allow flushing of the system with pure nitrogen. Measurements at saturation pressure were carried out by placing beakers with hydrocarbon in the housing. The lower drawing illustrate the transition state investigated.

saturation pressures were performed by placing beakers with hydrocarbon in the housing. Special care was taken in the cleaning of the system in between subsequent experiments.

Some experiments were carried out using a specially designed filmbalance for liquid–liquid interfaces as well as some initial experiments carried out with the R&K1 system.<sup>17</sup> This balance is optimized for the optical imaging, and the arrangement ensures that only the quartz housing and the water subphase are exposed to the hydrocarbon. Hence, the system can be easily cleaned and the reproducibility with both systems shows that there are no artifacts due to trace impurities or other contaminants. In addition the trough enables measurements at the macroscopic oil–water interface.

Figure 1b is a drawing illustrating the transition state investigated. The variation of the gas phase composition allows a gradual transition from the air–water interface to the macroscopic oil–water interface. The transition state resembles features of both interfaces and allows all techniques available for the air–water interface to be used.

For all measurements, the system was allowed first to equilibrate which usually required about 10 h. The system was flushed overnight before measurements were recorded. Figure 2 shows the time dependence of the surface pressure  $\pi$  with the exposure of the monolayer to a gas phase containing hydrocarbon. The most striking changes occur within the first 2 h. Figure 2 was recorded for the phospholipid DPPE and cyclohexane and is also representative for all investigated systems.

**2.2. Optical Characterization.** All relevant design features of the imaging ellipsometer used (Multiskop, Optrel FRG) are discussed in detail in ref 18. It is based on a null-ellipsometer in a laser, polarizer, compensator, sample, analyzer arrangement. For imaging purposes the photodiode is replaced by a CCD camera and an ultralong

(11) Lai, C. C.; Yang, S. H.; Finlayson-Pitts, B. J. *Langmuir* **1994**, *10*, 4637.

(12) Thoma, M.; Pfohl, T.; Möhwald, H. *Langmuir* **1995**, *11*, 2881.

(13) Gehlert, U.; Vollhard, D.; Brezeszinski, G.; Möhwald, H. *Langmuir* **1996**, *12*, 4892.

(14) Aveyard, R.; Binks, B. P.; Cooper, P.; Fletcher, P. D. *Adv. Colloid Interface Sci.* **1990**, *33*, 59.

(15) Aveyard, R.; Binks, B. P.; Fletcher, P. D.; MacNab, J. R. *Ber. Bunsenges. Phys. Chem.* **1996**, *100*, 224.

(16) Boublic, T.; Fried, V.; Hala, E. *The vapor pressure of pure substances*; Elsevier: London, 1973.

(17) Teppner, R.; Harke, M.; Motschmann, H. *Rev. Sci. Instrum.*, in press.

(18) Harke, M.; Teppner, R.; Schulz, O.; Orendi, H.; Motschmann, H. *Rev. Sci. Instrum.*, **1997**, *68* (8).

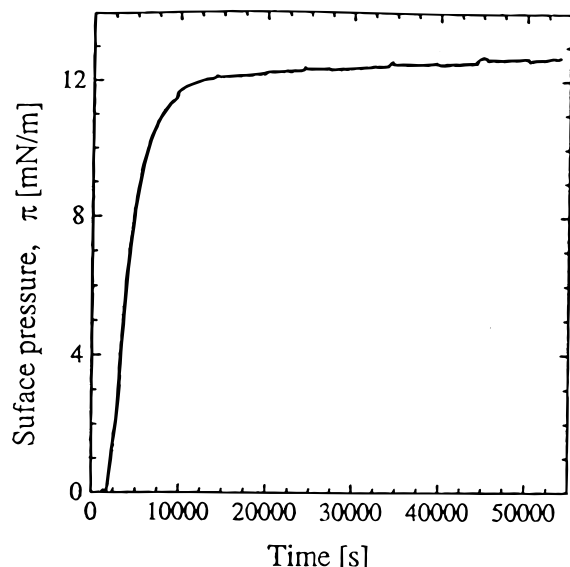


**Figure 2.** Surface pressure of DPPE as a function of time  $t$ . At  $t = 0$  the DPPE monolayer was exposed to a gas phase containing  $n$ -hexane. Similar features were observed for all hydrocarbons used.

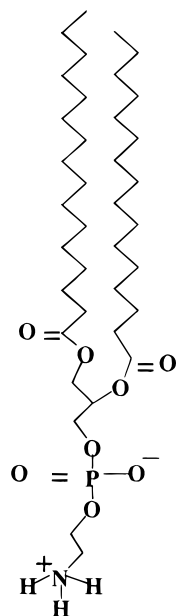


**Figure 3.** Chemical structure of the phospholipid  $D,L$ - $\alpha$ -dipalmitoylphosphatidylethanolamin, DPPE. The aliphatic tail determines the packing within the monolayer.

microscope objective with a working distance of 34 mm and a numerical aperture (NA) = 0.22 is inserted. A algorithm used for data analysis is described in ref 19.

**2.3. Materials.** The chemical structure of the phospholipid  $D,L$ - $\alpha$ -dipalmitoylphosphatidylethanolamine (DPPE) is presented in Figure 3. DPPE was purchased from Sigma-Aldrich and used as received.

The chemical structure of the hexadecanoic acid, 2,3-dihydroxypropyl ester (ESD-16), is presented in Figure 4. ESD-16 was purchased from Sigma-Aldrich and used as received.

All hydrocarbons were purchased from Sigma-Aldrich. Trace impurities are always a major concern in the investigation of interfacial properties. Some trace im-

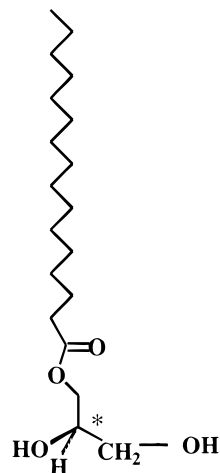


**Figure 4.** Chemical structure of the hexadecanoic acid, 2,3-dihydroxypropyl ester, ESD-16. The bulky headgroup determines the packing within the monolayer.

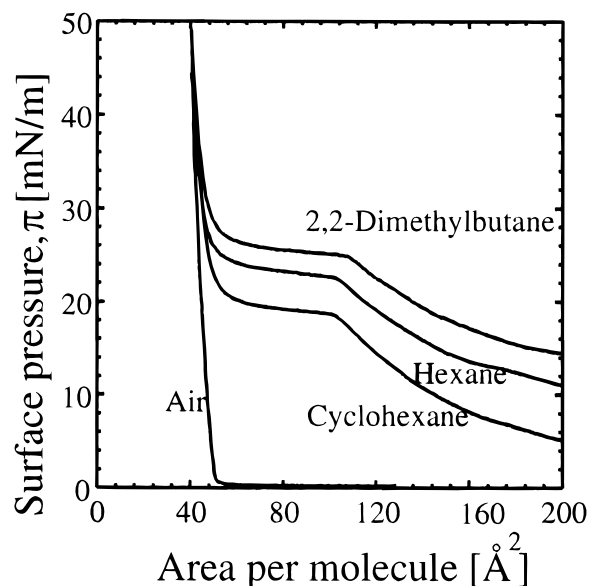


**Figure 5.**  $\pi,A$ -isotherm of the phospholipid DPPE at the air-water interface and in contact with a gas phase containing  $n$ -hexane, cyclohexane, and 2,2-dimethylbutane. The presence of the hydrocarbon in the gas phase induces a coexistence region. All isotherms were recorded at 22 °C and at saturation vapor pressure of the hydrocarbon.

purities possess a high affinity for the interface of interest, and thus the interface becomes enriched. These impurities are efficiently removed by the shaking of the hydrocarbon with water and subsequent decantation of the organic phase. This purification method is analyzed in ref 20.

### 3. Results and Discussion

**3.1.  $\pi,A$ -Isotherm. 3.1.1. DPPE:** The  $\pi,A$ -isotherm of DPPE recorded at 20 °C at the air-water interface is fairly simple and presented in Figure 5. During the compression of the monolayer a homogeneous liquid-condensed phase is formed at a molecular area of 52 Å<sup>2</sup>. Significant changes in the  $\pi,A$ -isotherm occur once the system is exposed to a gas phase containing hydrocarbon. Figure 5 presents the corresponding isotherms for cyclohexane,  $n$ -hexane, and 2,2-dimethylbutane. The most prominent feature is a newly formed plateau in the  $\pi,A$ -isotherm. The area per molecule at which the onset of the plateau occurs is fairly independent of the specific

(19) Harke, M.; Stelzle, M.; Motschmann, H. *Thin Solid Films* **1996**, 284, 412.

(20) Goebel, A.; Lunkenheimer, K. *Langmuir* **1997**, 13, 369.

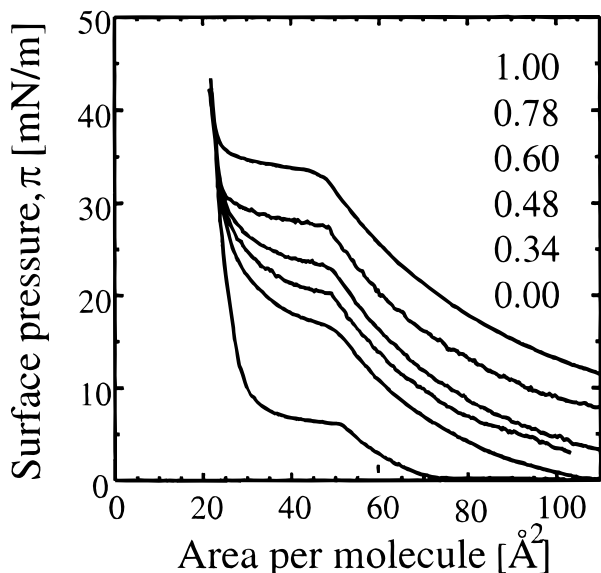


**Figure 6.** Influence of the *n*-heptane partial pressure on the corresponding isotherm of ESD-16. The prevailing partial pressure is normalized by its saturation pressure as indicated by the numbers in the graph.

isomer. Only a slight shift to higher areas per molecule is observed for 2,2-dimethylbutane, which might be attributed to its size. Furthermore all isotherms are shifted to higher surface pressures,  $\pi$ , and a correlation with the saturation vapor pressure,  $p_{\text{sat}}$ , of the hydrocarbon can be found; the  $p_{\text{sat}}$  values of the different hydrocarbons are 35.1 kPa cyclohexane, 16.2 kPa *n*-hexane, and 10.3 kPa 2,2-dimethylbutane.<sup>16</sup> The partial pressure determines the number of molecules which strike the surface per unit area and time. The liquid-condensed region is formed at a given molecular area which is independent of the presence and specific chemical nature of the hexane isomer.

To summarize, the presence of hydrocarbon in the gas phase induces the formation of new phases. The specific chemical nature of the hydrocarbon has only a minor impact on the features of the  $\pi, A$ -isotherm. The hydrocarbon is not incorporated in the liquid condensed phase of DPPE.

**3.1.2. ESD-16.** The influence of the partial pressure on the  $\pi, A$ -isotherm of ESD-16 was investigated using *n*-heptane. Figure 6 shows the corresponding isotherms recorded at 22 °C at different partial pressures of *n*-heptane. The prevailing partial pressure of *n*-heptane is normalized by its saturation vapor pressure as indicated in the inset of Figure 6. The first onset in the surface pressure at the air–water interface occurs at a molecular area of about 70 Å<sup>2</sup>. At a molecular area of 52 Å<sup>2</sup>, a coexistence region between a liquid condensed and liquid expanded phase is observed. The low compressibility of the liquid condensed phase causes a steep increase in  $\pi$  at low areas per molecule.

The presence of *n*-heptane in the gas phase does induce changes in the  $\pi, A$ -isotherm. As depicted in Figure 6, the onset of the surface pressure occurs at higher areas per molecule. There is still a coexistence region but it is shifted to higher surface pressures,  $\pi_c$ , and lower areas per molecule. The plateau value of the surface pressure,  $\pi_c$ , does not depend linearly on the partial pressure of the hydrocarbon. The liquid condensed phase is formed at a molecular area of 22 Å<sup>2</sup> and is independent of the prevailing *n*-heptane partial pressure. Hence, no hydrocarbon is incorporated in the liquid condensed phase.

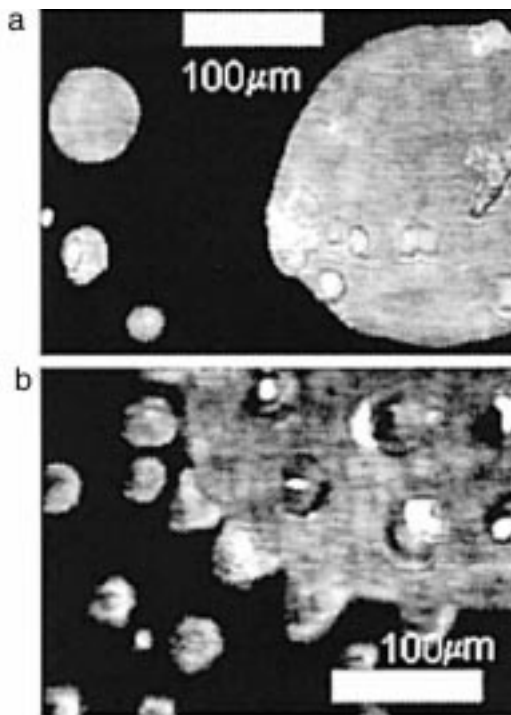


**Figure 7.** (a) Morphology of DPPE in the low-pressure region of the isotherm. There are two distinct phases in the low-pressure region of the isotherm. The very same features were observed within the homologous series of *n*-alkanes. The image was recorded at  $\pi = 10$  mN/m in a gas phase containing cyclohexane at its saturation vapor pressure and at a temperature of 22 °C. Microdroplets of hydrocarbon are formed on the domains. (b) The domains which are observed in the low-pressure region dissolve in the plateau of the  $\pi, A$ -isotherm. The growth of the new phase occurs in the center of the domain as well as at the edge.

**3.2. Imaging Ellipsometry. 3.2.1. DPPE:** The process of spreading usually leads to nonequilibrium structures of floating islands at the air–water interface. The shape of these nonequilibrium structures depends strongly upon the preparation process such as spreading agent and concentration of the solution etc. However, with the first onset in the surface pressure,  $\pi$ , a homogeneous phase of a liquid expanded monolayer is formed. In this region of the isotherm, ellipsometric images reveal a homogeneous phase with uniform reflectivity.

With the introduction of hydrocarbon in the gas phase, completely different features are observed. The onset in the surface pressure,  $\pi$ , does not lead to the formation of a uniform phase. Instead, imaging ellipsometry identifies two well-defined phases in the low-pressure region. Figure 7 shows the morphology of DPPE recorded in a cyclohexane atmosphere at a saturation pressure  $\pi_{\text{sat}}$ . Domains of a circular shape with uniform optical properties are embedded in a homogeneous matrix. Microdroplets form on the domains. Presumably, the microdroplets consist of a hydrocarbon which does not wet the underlying monolayer.

Further compression leads to the formation of a new phase in the plateau of the  $\pi, A$ -isotherm. The growth of a new phase occurs not only at the edge but also within the center of the domain as shown in Figure 7. A black matrix of a less densely packed monolayer separates the new from the old phase. The new phase consists of domains of circular shape. They vary in size of between 10 and 20  $\mu\text{m}$  and are significantly smaller than their counterparts at the air–water interface. This and the loss of contrast due to the presence of hydrocarbon in the gas phase makes it also more challenging for imaging

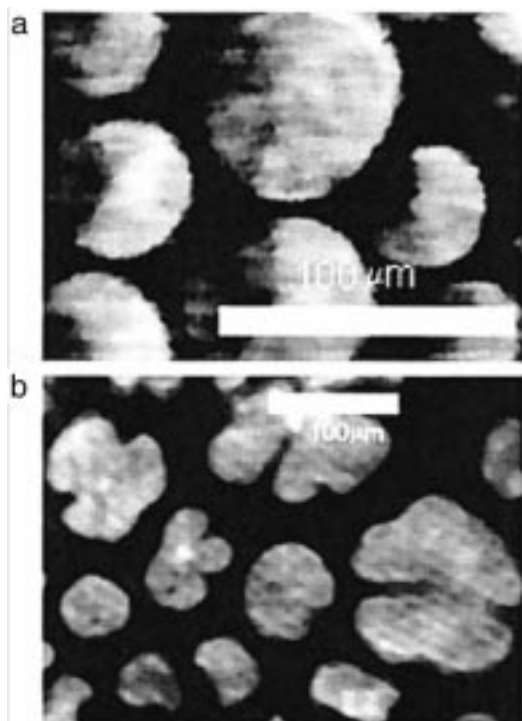


**Figure 8.** (a) Morphology of DPPE in the plateau of the isotherm under various hydrocarbons. Domains with circular shape and an internal order are observed. The molecule adopt a common azimuthal angle within each segment of the domain. The image was recorded for cyclohexane but it is also representative for other hydrocarbons: pentane, *n*-hexane, *n*-heptane, *n*-decane. (b) Within the homologous series the first change in morphology occurs with dodecane. In this case the domain lack an internal structure and the amphiphiles are organized with an upright orientation.

under an oblique angle of incidence. In addition, an internal structure with 6-fold symmetry is observed. The molecules are arranged in each segment with a common azimuthal angle. Hence the presence of hydrocarbon leads to the formation of a highly ordered crystalline state. Figure 8 shows a representative plot. The observed morphology is identical for the following hydrocarbons: cyclohexane, pentane, hexane, *n*-heptane, *n*-decane. The first deviations within the homologous series were observed with dodecane. Here the domains lack any internal structure as presented in Figure 8b. The molecules are orientated upright or an azimuthal isotropic molecular arrangement is adopted.

**3.2.2. ESD-16.** At the air–water interface, ESD-16 forms domains of a circular shape as presented in Figure 9a. A remarkable feature is an internal structure with 7-fold symmetry. In the majority of cases a common intersection point is located in the center of the domain, but in some instances the intersection point is observed at the edge of the domain. The latter is of a cardioid shape and quite frequently possesses less than seven segments. The structure and morphology were investigated in detail in ref 13. In each segment the molecules possess an identical azimuthal angle  $\phi$  and there is a discontinuity in  $\phi$  between adjacent segments. Under *n*-heptane at saturation pressure, the morphology of ESD-16 displays completely different features as illustrated in Figure 9c. At a hydrocarbon partial pressure close to saturation, the domains adopt a dendritic shape and lack any internal structure. The dendritic shape of the domains does not change during the course of the experiment (24 h), which might be explained in terms of a significant decrease in

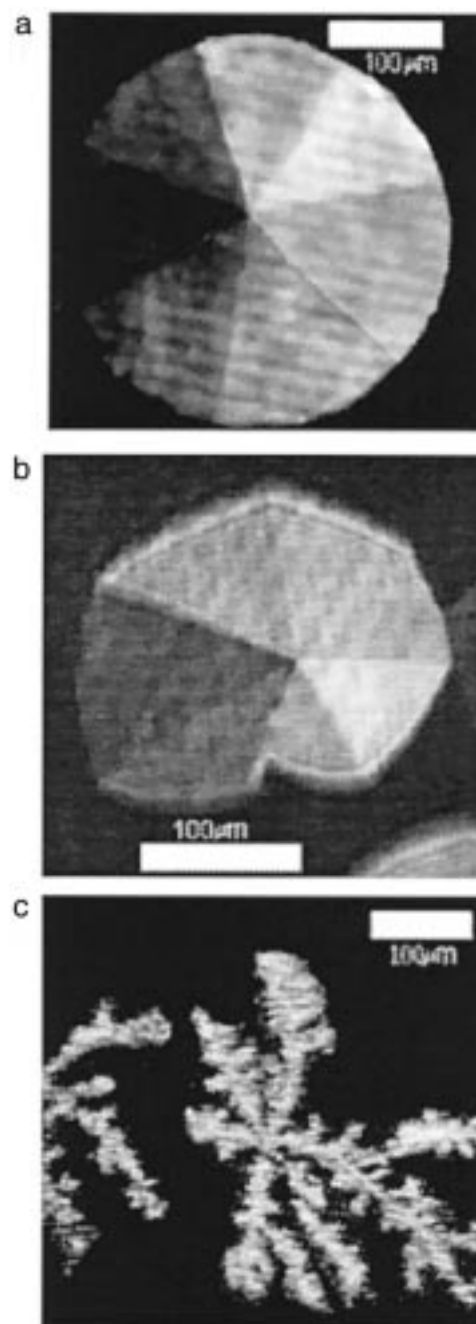


**Figure 9.** (a) Ellipsometric image of domains of ESD-16 recorded at the air–water interface. The domains are of circular shape and possess a 7-fold internal symmetry. Each segment possesses a uniform reflectivity and in the majority of cases there is a common intersection point in the center of the domain. (b) Morphology of the domains in the coexistence region of ESD-16 recorded at 22 °C and a partial pressure of heptan  $p = p_{\text{sat}}$ . (c) Morphology of ESD-16 recorded in contact with a gas phase containing *n*-heptane at its saturation vapor pressure. Dendritic domains with no internal structure are observed. The observed features do not change within 24 h.

line tension. Partial pressures below saturation,  $p_{\text{sat}}$ , preserve the internal structure of the domains. A representative image is shown in Figure 9b, which was recorded at a partial pressure of 0.6  $p_{\text{sat}}$ . All domains have lost their circular shape. In addition, a dip at one segment is observed which in some cases joins the intersection point of all segment boundaries at the center of the domain.

Nonequilibrium structures under a gas phase containing hydrocarbon produced under a fast compression interest-

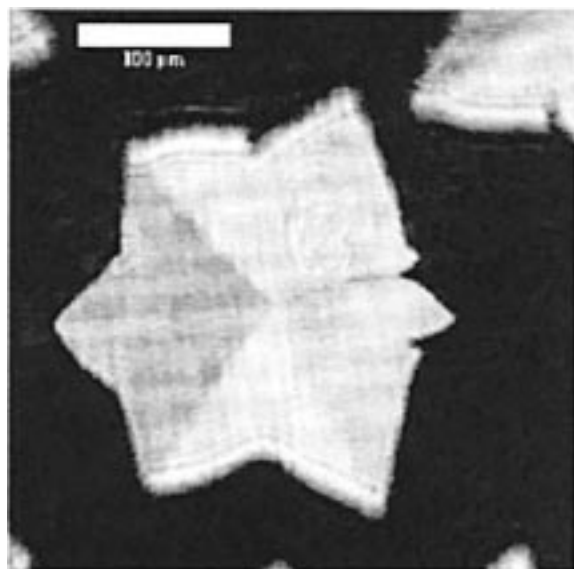


**Figure 10.** Nonequilibrium of ESD-16 produced by a fast monolayer compression in contact with *n*-heptane vapors. Contrary to the air–water interface, each arm consists of two regions of different reflectivity. The growth of the domain is in the direction of the boundary of two segments.

ing features compared to their counterparts at the air–water interface. Nonequilibrium structures at the air–water interface are of dendritic shape. Each finger possess its own unique reflectivity different from adjacent segments. The growth of each domain is directed to the half-angle of a segment.<sup>21</sup> Under hydrocarbon vapors each arm consists of two regions of a different reflectivity as shown in Figure 10. Hence, in this case the growth of the domain is governed by the direction of the boundary of two segments.

#### 4. Summary and Conclusions

The influence of a gas phase containing various hydrocarbons at well-defined partial pressures on insoluble monolayers of DPPE and ESD-16 was investigated by surface tension measurements and imaging ellipsometry. The latter provides information on a mesoscopic length scale. Different isomers of hexane demonstrate that the

specific shape of the molecules has only a minor impact on the  $\pi, A$ -isotherm as well as on the observed morphology.

In the case of DPPE, the presence of a hydrocarbon induces a coexistence region in its  $\pi, A$ -isotherm. In the plateau region domains of circular shape with an internal 6-fold symmetry are observed. The morphology is in this case independent of the hydrocarbons present (even aromatic ones). Within each segment of the domains, the molecules possess a common azimuthal angle  $\phi$ .

The liquid condensed phase is formed at a given molecular area independent of the partial pressure and the specific hydrocarbon used. Hence the hydrocarbon is not incorporated within the liquid condensed phase. During compression it is squeezed out of the monolayer and forms droplets on it. Two phases were observed within the low-pressure region. The tilt angle of the monolayer depends on the presence of hydrocarbon and is specific to the shape of both amphiphile and hydrocarbon.

The coexistence region observed with ESD-16 at the air–water interface is preserved in contact with hydrocarbon. However, the onset of the plateau is shifted toward lower molecular areas with increasing hydrocarbon partial pressure. At the air–water interface, domains with seven segments of uniform reflectivity are observed. At the saturation vapor pressure of *n*-heptane, dendritic domains are formed and the inner structure of the domains is lost. The hydrocarbon is incorporated which leads to an upright organization of amphiphiles. There is a continuous transition between both states with increasing partial pressure. At a partial pressure below saturation, the circular shape of the domains becomes deformed and the common intersection point of all the segment is quite frequently shifted to the edge of the domain.

Results on the interaction of monolayers with molecules from a gas phase contribute to the understanding of the molecular organization of amphiphiles at the air–water and oil–water interface. With our arrangement it is possible to use all established analytical tools suitable for the investigation of the air–water interface. The conditions are well defined with a uniform interaction in time and space, and the partial pressure of the hydrocarbon can be controlled.

**Acknowledgment.** The authors thank Professor H. Möhwald for encouraging discussions and his support and also Dr. Martina Bree for helpful discussions.

LA970938E

(21) Gehlert, U.; Weidemann, G.; Vollhardt, D. *J. Colloid Interface Sci.* **1995**, *174*, 392.